Progress In Electromagnetics Research C, Vol. 134, 197–209, 2023

Resistance Loaded UWB MIMO with Enhanced Isolation for S and C Band Applications

Aditi Sharma[1, *], Sumit K. Gupta[1], Robert Mark[2], Bhawna Shukla[1], and Soma Das[1]

Abstract—A hexagon-shaped fractal ultra-wideband (UWB) Multiple Input Multiple Output (MIMO) antenna is proposed in this paper for S (2 GHz to 4 GHz) and C (4 GHz to 8 GHz) band applications. The proposed design consists of two microstrip fed radiating elements of dimension $82 \times 44 \times 1.6\,\text{mm}^3$. One rectangular stub and four resistance loaded stubs are introduced in the ground plane to reduce the mutual coupling between the radiators. These decoupling structures reduce the notches and enhance the isolation from −5 dB to −20 dB for the entire frequency range from 2.3 to 7.4 GHz. The performance characteristics and diversity parameters are also investigated which show the values of ECC < 0.004, DG > 9.96, CCL < 0.4, and MEG < 3 dB, and it is concluded that the proposed design is a good candidate for UWB MIMO antenna. The proposed design is fabricated and tested which shows the close agreement between the simulated and measured results.

1. INTRODUCTION

As per the increased need of communication devices, the requirement of the high data rate, limited power levels for high quality of data transmission, pattern diversity, channel capacity, fabrication ease, compact size, and cost efficiency is also increased [1–4]. Single Input Single Output (SISO) systems are struggling to fulfil the requirements of the modern era because of their limited bandwidth, multipath fading, etc. UWB MIMO antenna is a good candidate for achieving the above requirements, and therefore this grabs the attention of the researchers. Compact size of the MIMO antenna is the main concern of the researchers, but it generates mutual coupling between the radiators since the port-to-port distance of the radiator decreases [5]. This mutual coupling causes the degradation of diversity parameters, efficiency, and the gain of the antenna [6]. Various techniques and methods for reducing the mutual coupling are proposed in the literatures. Some of them are orthogonal placement of antenna with an L-shaped stub and different shapes of slots in the ground plane [7, 8], introduction of Electromagnetic Band gap (EBG) [9], impact of metamaterial [10], introduction of neutralization line [11–13], Defected Ground Structures (DGSs) [14–16], etc. Fractal shaped defects are also very useful in reducing mutual coupling; some of the applications are complementary modified Minkowski fractal [17], radiator with Sierpinski Knopp fractal [18], H-shaped fractal [19], Hilbert fractal [22], and many more. The modification in a feedline/stub is another way to enhance the isolation, i.e., step feedline with DGS structures [20], tapered feedline and tapered patch [21], spider-shaped radiator with Y-shaped stub [23], Swastik shaped hepta-band antenna [24], decoupling dielectric stub (DDS) [26–28], I-shaped stub with inverted L-shaped branch to produce a T-like branch on ground [29], etc. Even reconfiguration of frequency is also possible with the help of diode [25]. Apart from the above methods, the use of lumped elements such as capacitance and resistance for mutual coupling reduction is also implemented to enhance the isolation of MIMO antenna by the researchers [30, 31]. The ease of fabrication and considerable amount of isolation

Received 22 March 2023, Accepted 12 June 2023, Scheduled 12 July 2023

* Corresponding author: Aditi Sharma (sharma.aditi1610@gmail.com).

[1] Department of ECE, SoS of Engineering & Technology, Guru Ghasidas Vishwavidyalaya Bilaspur, India. [2] Antigone Solutions Pvt Ltd, Bangalore, India.

enhancement are observed by implementing stub and lumped element in MIMO which encourages the use of resistance loaded stub as proposed in the next section.

In this paper, a compact 2 element hexagon fractal-shaped MIMO system is presented for S-band and C-band applications. CST 2018 is used for the simulation and verification of the antenna. After the simulation the fabrication is done and tested with the help of vector network analyser (VNA) by using radiation patterns measurement setup. Two hexagonal fractal antennas are placed in parallel with the dimension of $82 \times 44 \times 1.6\,\text{mm}^3$. The operating range of the antenna is 2.3 to 7.4 GHz with an isolation of more than -20 dB. The diversity parameters such as envelope correlation coefficient (ECC), mean effective gain (MEG), channel capacity loss (CCL), and diversity gain (DG) are calculated for verifying the result of the proposed antenna.

2. MATERIALS AND METHODS

2.1. Design Parameters

Figure 1 shows the proposed UWB MIMO antenna with the resistance loaded stub. The proposed antenna is fabricated on an FR-4 substrate with the thickness 1.6 mm, dielectric constant $\varepsilon_r = 4.4$, and tangent loss $\tan\delta = 0.023$. A 50 Ω microstrip feedline is used to feed the nested loop hexagonal fractal.

The design parameters of the proposed antenna are as follows: length and width of antenna are $Lsub = 44$ mm and $Wsub = 82$ mm respectively; length and width of the feedline $(wf) = 2.84$ mm and $(Lf) = 11.41$ mm; length and width of the central stub are $(Lstub) = 38$ mm and $(Wstub) = 2$ mm; length and width of the resistive stub are $lrstub = 33$ mm and $wrstub = 2$ mm, respectively with the resistance $R1$, $R2$, $R3$, and $R4 = 200\,\Omega$; separation between the antenna (gap) = 6 mm with the reduced ground $(Lground) = 10$ mm.

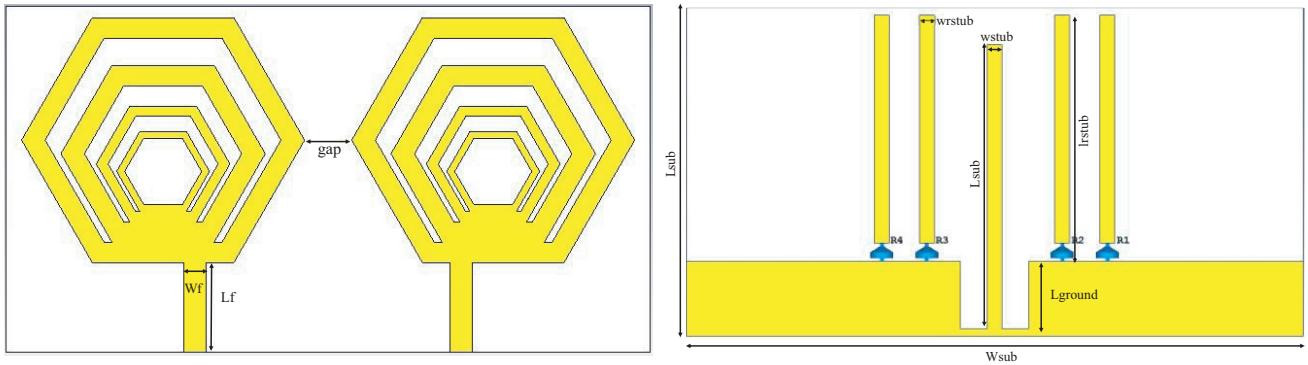

Figure 1. Proposed fractal MIMO. (a) Front view. (b) Back view.

2.2. Design Evolution of Single Element

The proposed antenna is based on the concept of self-repeating and self-similarity geometry, and the design is initiated with the single hexagonal ring (initiator) monopole antenna of side 15 mm which resonates at three frequencies, but the dominating frequency is 5 GHz. The further stages are obtained by using equation below:

$$S_{n+1} = \theta \cdot S_n \tag{1}$$

Here n is the number of iteration stages = 1, 2, 3; S is length of the side; and θ is the scale factor for the proposed design $\theta = 0.734$ [31]. The gap between the fractal arms and the width of the ring is optimized to achieve wideband response from multiband characteristics. The effects of addition of each iteration is shown in Figure 2(a), and the effect of ground reduction is shown in Figure 2(b). The response of the optimized fractal after the ground reduction is shown in Figure 3.

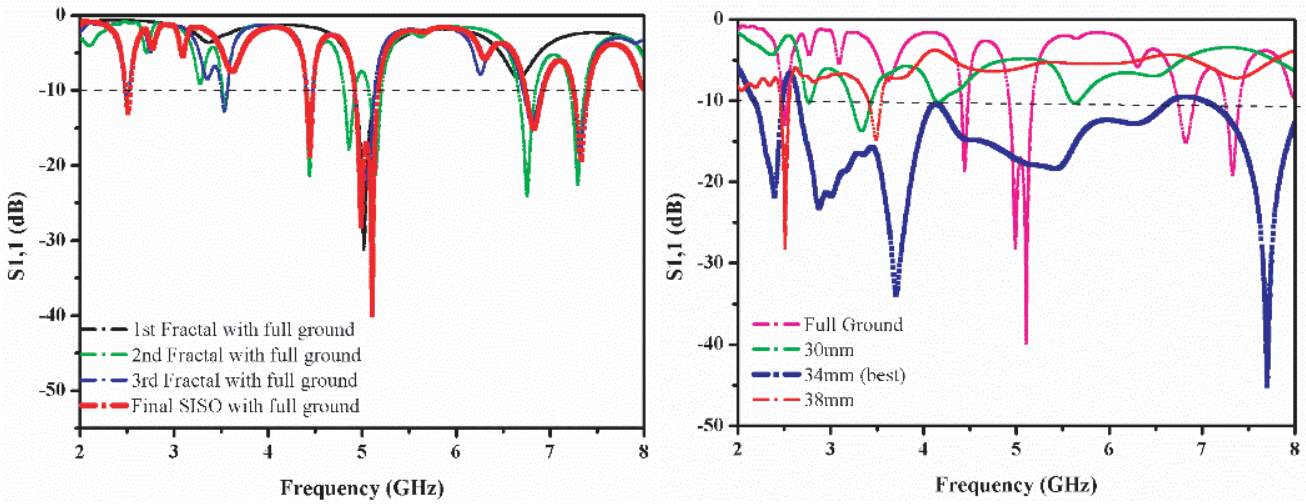

Figure 2. (a) S_{11} of addition of each iteration. (b) S_{11} of reduced ground.

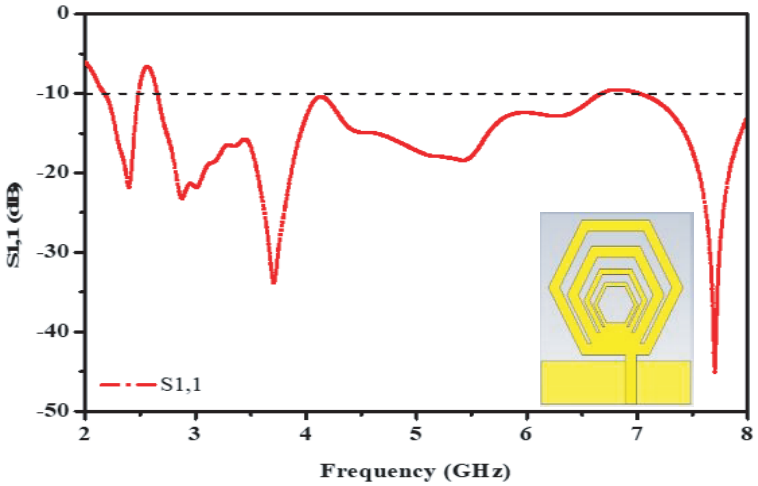

Figure 3. S_{11} of single fractal of the proposed design with reduced ground.

For further improvement in the bandwidth and channel capacity, the single element antenna is extended to 2-element MIMO; however, the mutual coupling starts to affect the performance of fractal as evidenced by the S parameters shown in Figure 4. To reduce this mutual coupling and enhance the performance of the MIMO antenna, decoupling structures such as stub and resistance loaded stub are introduced in the ground plane.

2.3. The Evolution Process of the Proposed MIMO Design

The proposed design evolution starts with stage 1 which shows the formation of single hexagonal fractal antenna with reduced ground as shown in Figure 3. Stage 2 is the extension of single fractal antenna into 2×1 MIMO by placing it side by side as shown in Figure 4. Further in stage 3, an inset cut grounded stub is introduced at the center of the reduced ground as shown in Figure 5 (figure inset). The wide band response from 2.1 GHz to 7.52 GHz with the notches (2.49 GHz–2.72 GHz, 3.43 GHz–4.04 GHz) is obtained by optimizing the position, width ($Wstub$), and height ($Lstub$) of the stub. Along with introduction of notches, the considerable amount of improvement in S_{21} is also observed.

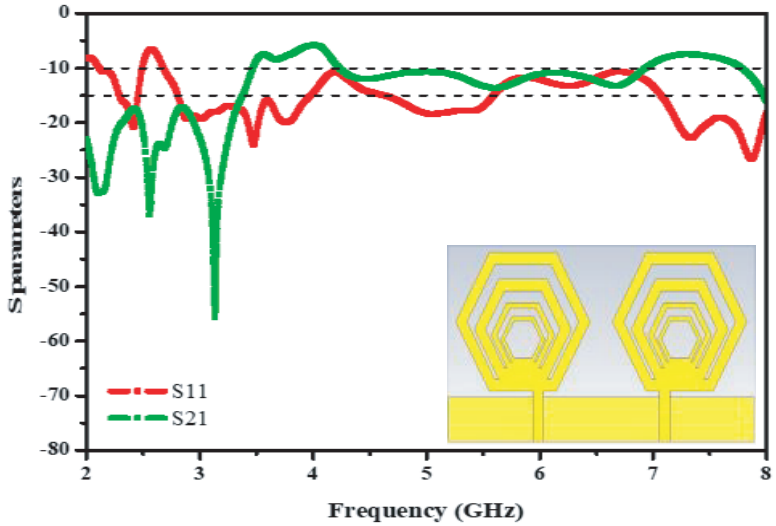

Figure 4. S-parameters of 2×1 MIMO.

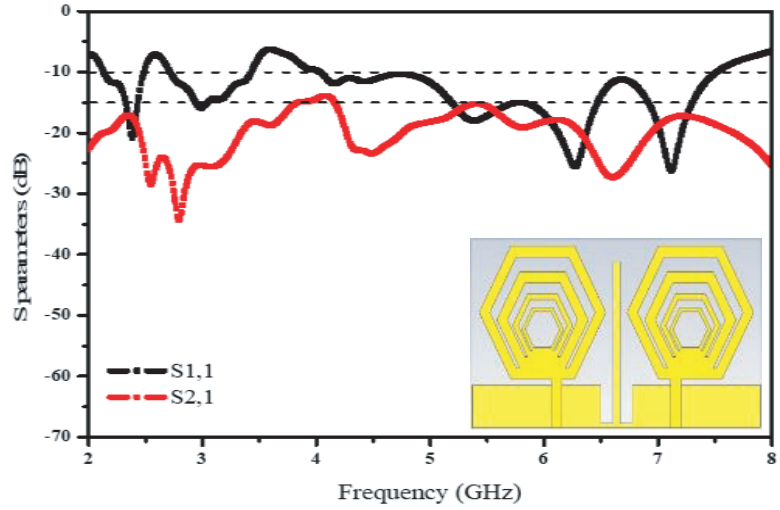

Figure 5. S parameters of the 2×1 MIMO antenna with reduced ground and stub.

The introduction of stub in between the radiators extends the path of current flow which helps in reduction mutual coupling up to −15 dB.

After the optimization of the central stub, in final stage, four more stubs with resistance are introduced in the reduced ground as shown in Figure 1(b) which gives the wideband from 2.36 GHz to 7.45 GHz and is obtained by suppressing the notches (2.49–2.72 GHz and 3.43–4.04 GHz). The optimization of the position of the resistance loaded stub and the value of resistance are shown in Figure 6. It is observed from Figure 6 that the isolation is improved from −15 dB to −20 dB in the entire range due the increased resistance of the stub as shown in Figure 1(b). These resistance loaded stubs provide better isolation and impedance matching to this 2×1 MIMO system.

The plot of surface current distribution is used for further analysis of the performance of the proposed design. The comparison between surface current distributions of 2×1 MIMO antenna with and without decoupling structure is shown in Figure 7 at frequencies 2.86 GHz, 4.22 GHz, 5.83 GHz, 7.07 GHz. This comparison shows that the introduction of the stub and the resistance loaded stub reduces the coupling of the current between the antenna elements.

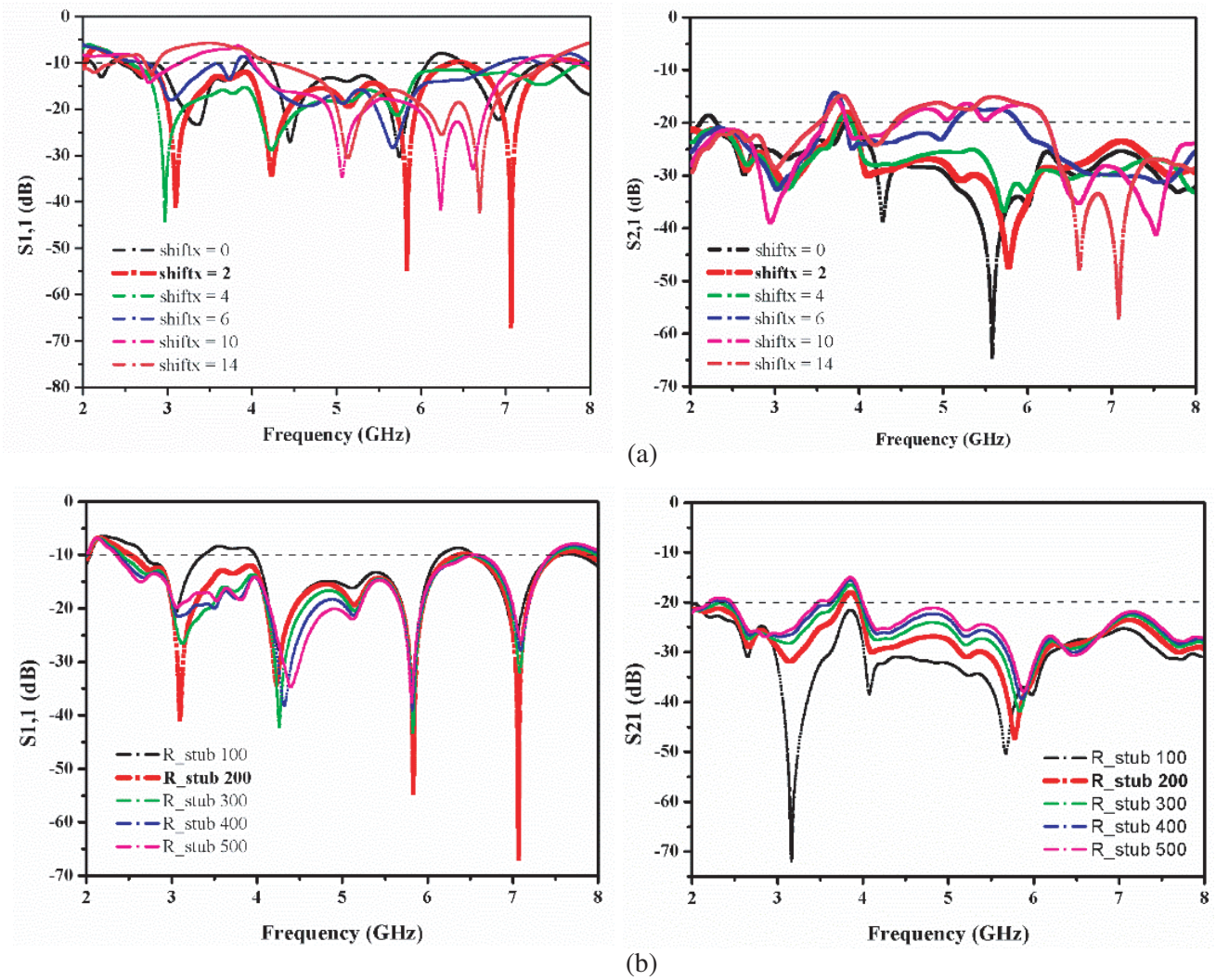

Figure 6. (a) S-parameters of optimized position of resistive stub. (b) S-parameters of optimized value of resistance.

2.4. Equivalent Circuit Model

The proposed design is further analyzed using the equivalent circuit of the proposed MIMO antenna. Advanced Design System is used to optimize and tune the required circuit. The UWB response of the proposed design consists of parallel R-L-C circuits which are connected in series with port impedance, resistance and capacitance. The proposed circuit is shown below in Figure 8(a), and the comparison

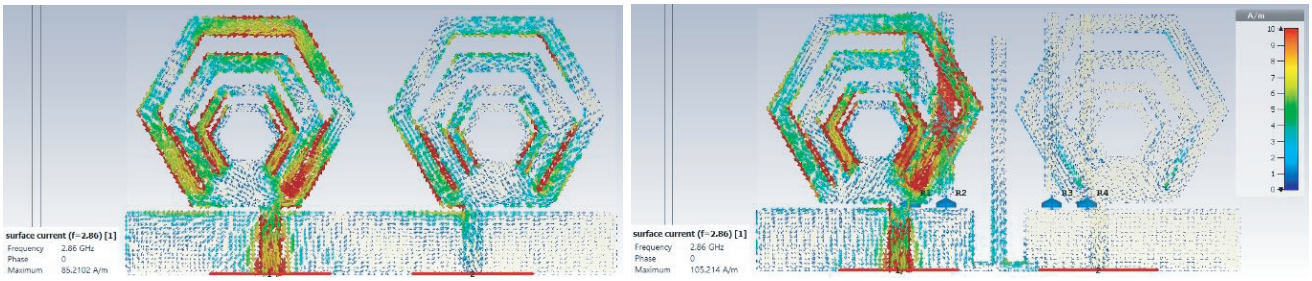

(a)

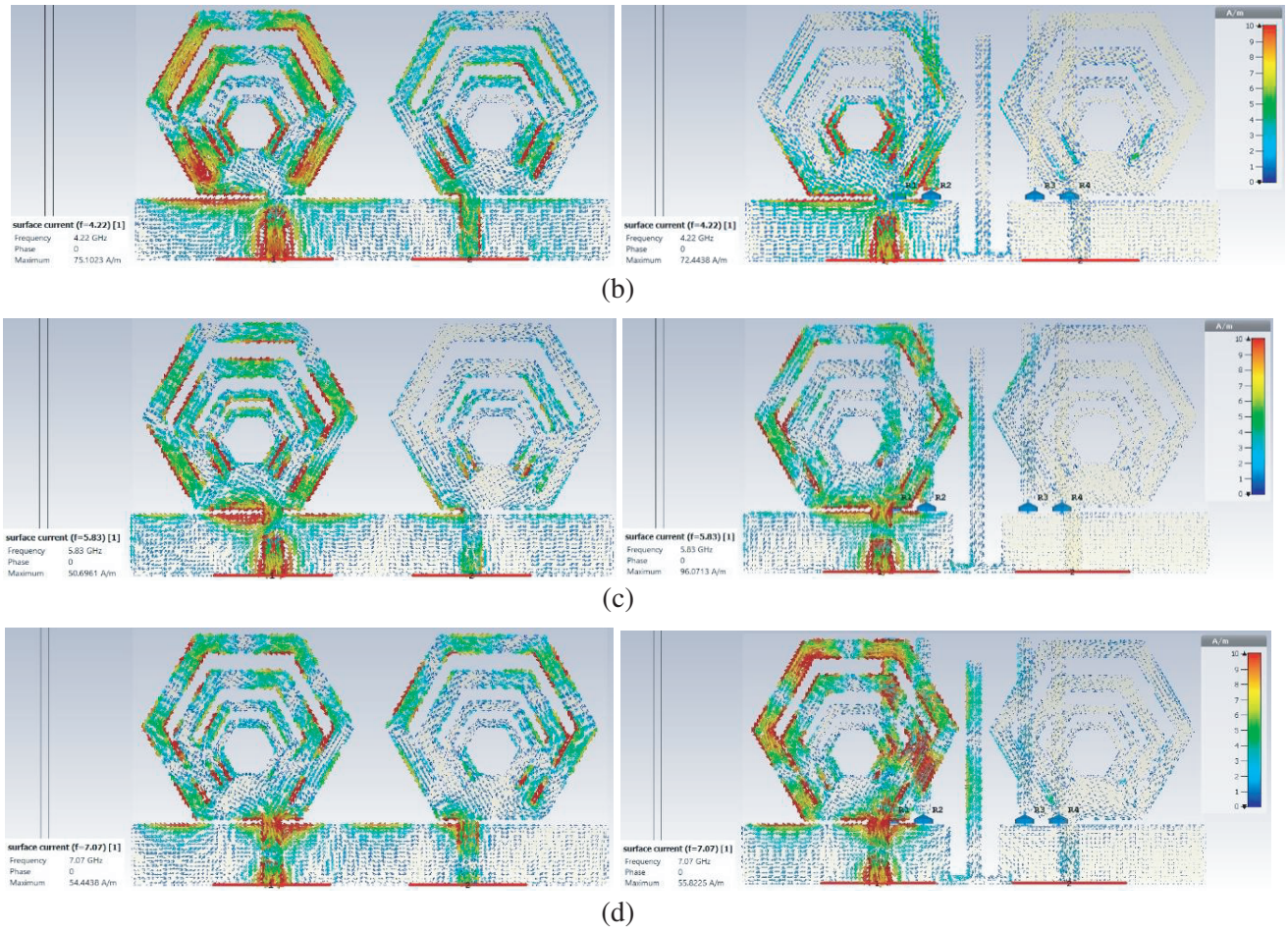

Figure 7. Surface current distribution at frequency (a) 2.86 GHz, (b) 4.22 GHz, (c) 5.83 GHz, (d) 7.07 GHz.

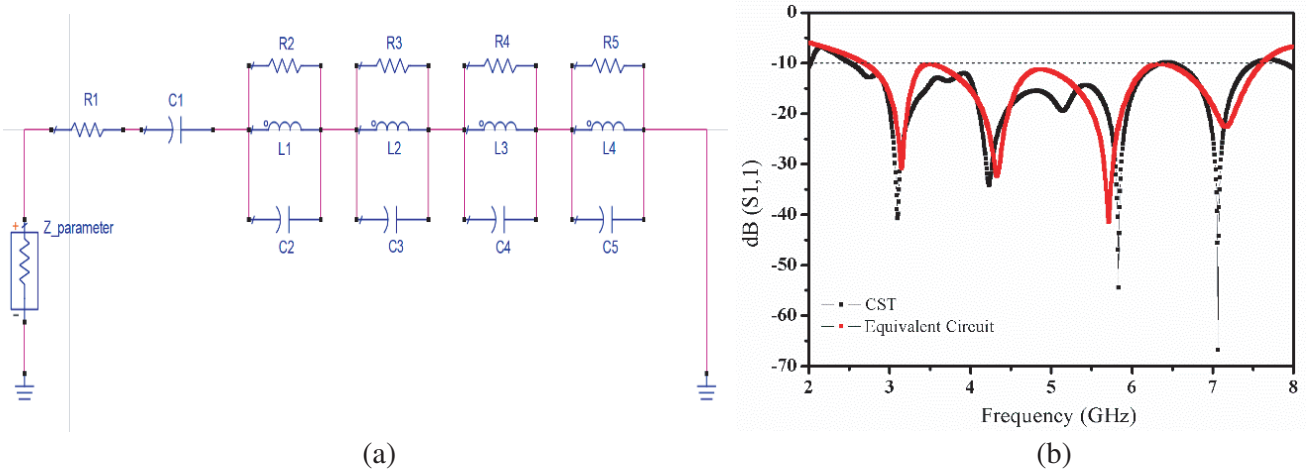

Figure 8. (a) Equivalent circuit of proposed antenna. (b) Comparison between the response of equivalent circuit (S_{11}) and CST output.

between the response of equivalent circuit (S_{11}) and CST output is shown in Figure 8(b). The values of component are given below:

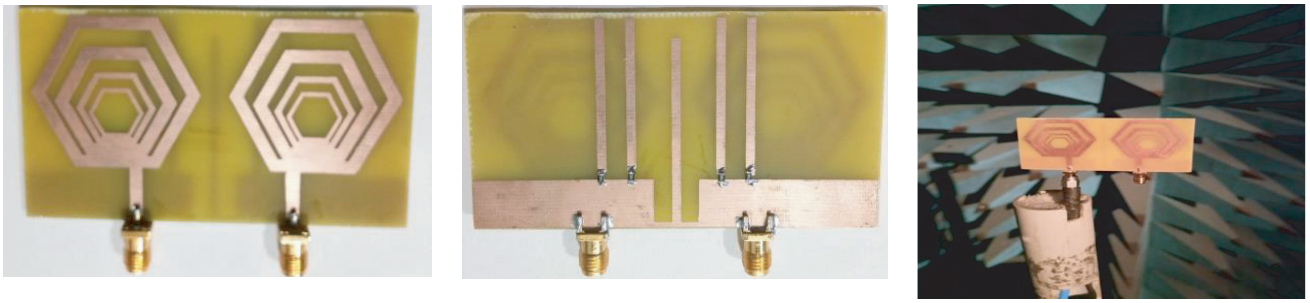

(a) (b) (c)

Figure 9. Images of fabricated prototype. (a) Front view, (b) Back view, and (c) testing using vector network analyzer.

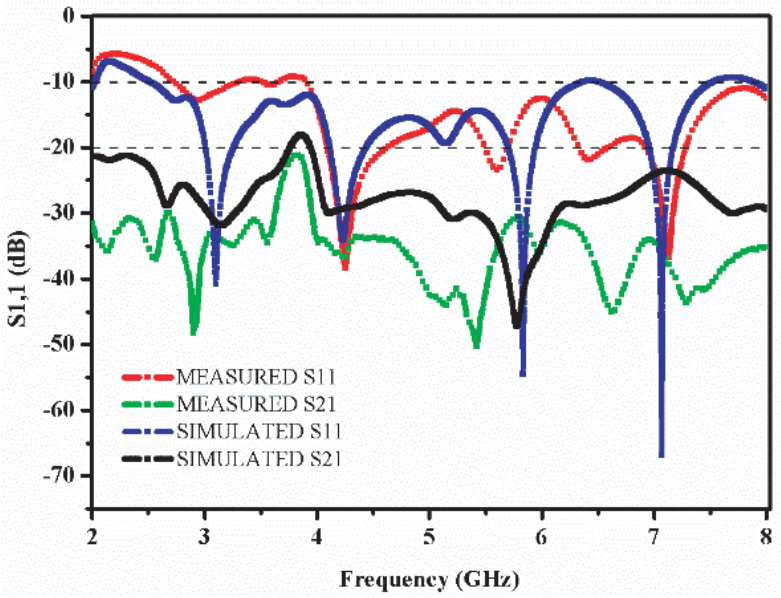

Figure 10. Comparison of simulated and measured S-parameters of proposed MIMO.

$C1 = 1.54\,\text{pF}$, $C2 = 14.0086\,\text{pF}$, $C3 = 5.5\,\text{pF}$, $C4 = 7.199\,\text{pF}$, $C5 = 3.11\,\text{pF}$, $L1 = 0.166\,\text{nH}$, $L2 = 0.121\,\text{nH}$, $L3 = 0.162\,\text{nH}$, $L4 = 0.13\,\text{nH}$, $R1 = 30.9\,\Omega$, $R2 = 35.45\,\Omega$, $R3 = 49\,\Omega$, $R4 = 42\,\Omega$, $R5 = 67.165\,\Omega$.

3. RESULTS AND DISCUSSION

The optimized design is fabricated and tested for experimental verification using a two-port vector analyzer (Agilent N5247A). The fabricated design along with measurement setup is shown in Figure 9, and the comparison between fabricated and measured S parameters is shown in Figure 10.

The S parameters of the fabricated antenna shows the improved value of isolation and impedance matching in the entire range of WLAN application. An anechoic chamber is used to measure the far field radiation patterns of the proposed 2×1 MIMO at frequencies of 3.1 GHz, 4.2 GHz, 5.8 GHz, 7.1 GHz (Figure 11). These radiation patterns show the near omnidirectional behavior of antenna in both the E-plane and H-plane with small cross polarization except at 3.1 GHz.

The MIMO antenna performance can be investigated by analyzing different diversity parameters such as ECC, DG, MEG [32], and CCL [33].

ECC is used to describe the isolation of the antenna system and the correlation between the

radiating elements. The radiation patterns of the antenna elements are correlated with each other. The amount of interference between the radiating signals is evaluated using S parameters when all the ports are simultaneously excited. For ideal condition its value is 0, but for the practical application ECC < 0.5 is considered an uncorrelated MIMO system. The mathematical representation is given by:

$$ECC = \frac{\left|S_{11}^{*}S_{12} + S_{21}^{*}S_{22}\right|^{2}}{\left(1 - |S_{11}|^{2} - |S_{21}|^{2}\right)\left(1 - |S_{22}|^{2} - |S_{12}|^{2}\right)} \tag{2}$$

Here S_{11}, S_{22} are the return losses at port 1 and port 2, and S_{21} and S_{12} are the isolation parameters. For the proposed fabricated design, the value of ECC less than 0.004 is shown in Figure 12(a).

DG is the measure of average signal to noise ratio of the radiating element. For the ideal condition its value should be 10 dB, and for proposed design its value is more than 9.96 which is a practically considerable amount as shown in Figure 12(b) and is calculated using formula:

$$Diversity\ Gain = 10\sqrt{1 - |ECC|^{2}} \tag{3}$$

The channel capacity of the antenna is increased with the increase in the number of radiators; however, the channel capacity loss is also increased due to the addition of correlation factor between the antenna

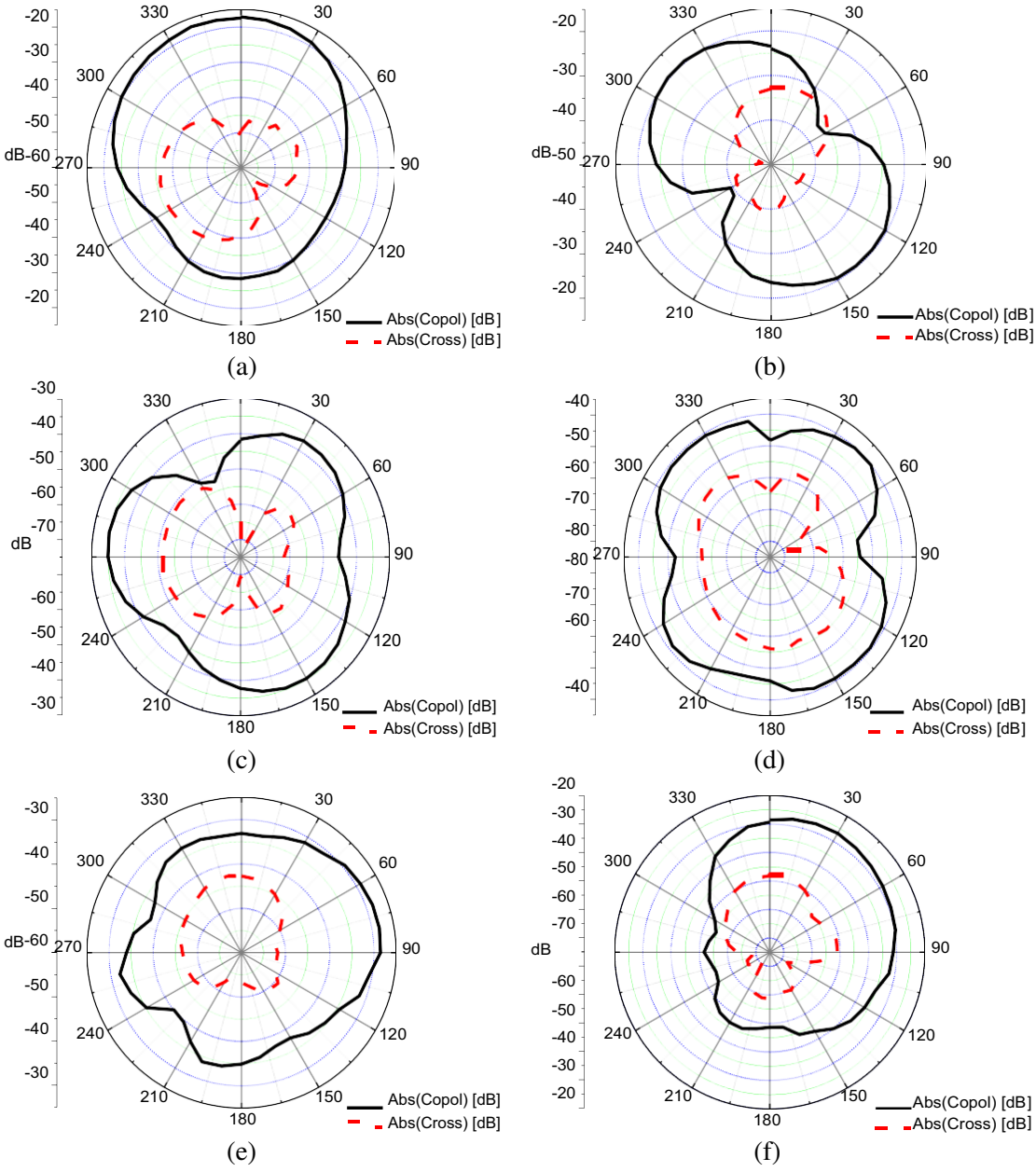

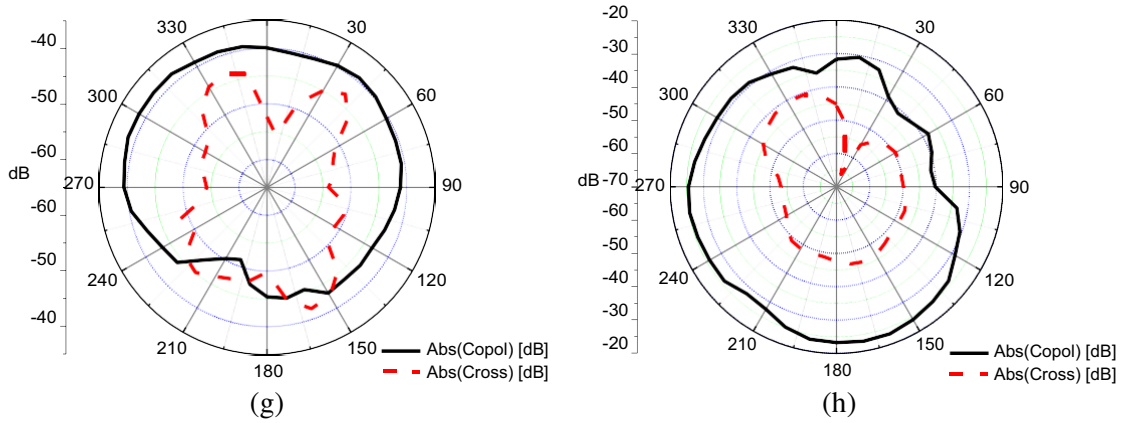

(g) (h)

Figure 11. The measured far field radiation patterns. (a) 3.1 GHz, phi = 0. (b) 3.1 GHz, phi = 90. (c) 4.2 GHz, phi = 0. (d) 4.2 GHz, phi = 90. (e) 5.8 GHz, phi = 0. (f) 5.8 GHz, phi = 90. (g) 7.1 GHz, phi = 0. (h) 7.1 GHz, phi = 90.

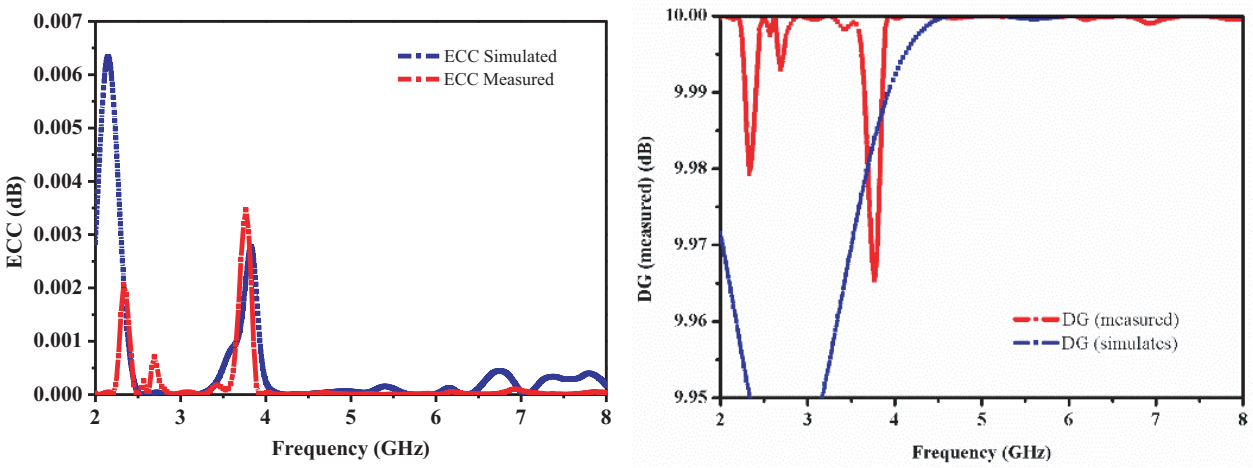

(a) ECC (b) DG

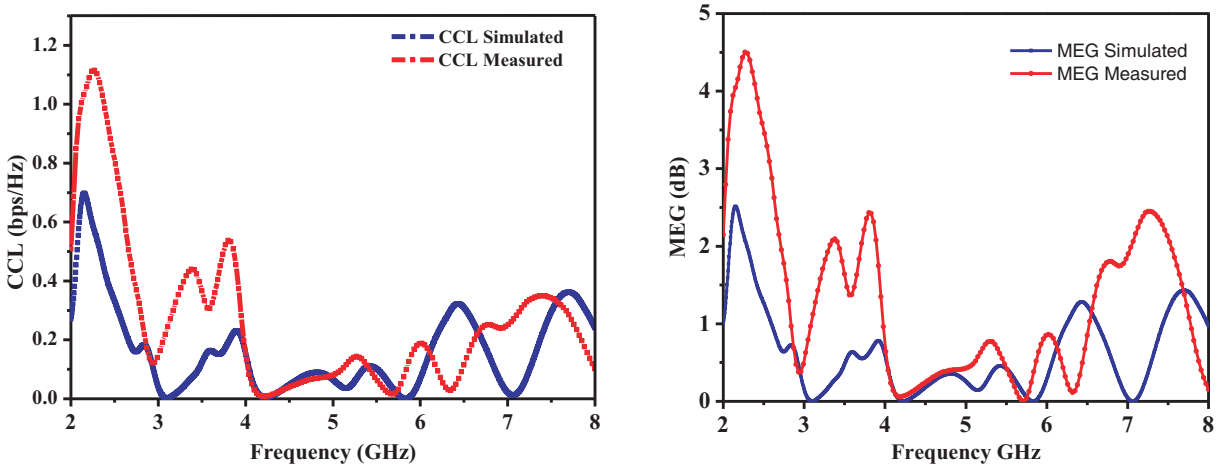

(c) CCL (d) MEG

Figure 12. (a) Comparison of ECC by S parameters, measured and simulated. (b) Comparison of DG by S parameters, measured and simulated. (c) Comparison of CCL by S parameters, measured and simulated. (d) Comparison of MEG by S parameters, measured and simulated.

elements. CCL is defined as the rate of data lost and transmitted fairly. It should be less than 0.4 bits/s/Hz for good performance of the MIMO antenna. The plot for the proposed design is shown in Figure 12(c). Its value can be calculated using the formula:

$$C_{loss} = -\log_2 \left|\Psi^R\right| \tag{4}$$

Here,

$$\Psi^R = \begin{bmatrix} \rho_{11} & \rho_{12} \\ \rho_{21} & \rho_{22} \end{bmatrix} \tag{5}$$

and

$$\rho_{ii} = \left(1 - |S_{ii}|^2 - |S_{ij}|^2\right) \quad \text{and} \quad \rho_{ij} = -\left(S_{ii}^* S_{ij} + S_{ji}^* S_{ji}\right) \quad \text{for} \;\; i, j = 1 \text{ or } 2 \tag{6}$$

Table 1. Comparison of proposed design with published literature.

Ref.	Dimension	Bandwidth	Edge to edge spacing	Technique	DG	ECC	Isolation (dB) better than	Material
[17]	22 mm × 28 mm	3.1–10.6 GHz	8 mm	Complementary modified Minkowski fractal	> 9.98	< 0.05	−17.07	FR-4
[24]	82 mm × 40 mm	Multiband 0.95–1.02 GHz, 1.73–1.79 GHz 2.68–2.85 GHz, 3.66–3.7 GHz 4.20–4.40 GHz, 5.50–5.65 GHz 5.93–6.13 GHz	5 mm	No additional coupling method	Not Reported	< 0.05	−17	FR-4
[34]	25 mm × 25 mm	2.97–13.8 GHz	Not reported	Stub	> 9.97	< 0.05	−15	FR-4
[35]	85 mm × 50 mm	2–9.5 GHz	Not reported	No additional coupling method	Not reported	< 0.03	−20	FR-4
[36]	41 mm × 99.4 mm	4.3–11.6 GHz	Not reported, centre tocentre (54.4 mm)	DGS	> 9.99	< 0.007	−17.9	FR-4
[37]	23 mm × 60 mm	2.65–11.6 GHz	Not reported	Stub	> 9.98	< 0.01	−15	FR-4
[38]	22 mm × 44 mm (2 port), 44 mm × 44 mm (4 port)	2.88–15.76 GHz, 2.84–15.88 GHz	Not reported	Orthogonal placement, isolated ground	> 9.95	< 0.01	−22, −15	Rogers RT Duroid5880
[39]	25 mm × 48 mm	2.57–19.15 GHz	Not reported	Orthogonal placement	> 9.95	< 0.006	−20	Rogers RT Duroid5870
Proposed Work	**44 mm× 82 mm**	**2.3 to 7.4 GHz**	**6 mm**	**Stub, resistance loaded stub**	**> 9.96**	**< 0.004**	**−20**	**FR-4**

MEG is the calculated value of the amount of electromagnetic power received by the antenna.

It is also defined as the ratio of mean received power to mean incident power of the antenna. The MEG can be calculated using equation

$$MEG_i = 0.5\left(1 - \Sigma_{j=1}^{k}\left|S_{ij}\right|^2\right) \tag{7}$$

Here, k is the number of antennas, and i is the antenna number for which MEG is calculated. The value of MEG must be less than 3 dB for better performance of the MIMO system. Figure 12(d) shows the MEG response of the proposed MIMO system which is less than 3 dB.

The proposed antenna design exhibits a good performance characteristic over the entire frequency range of 2.3 to 7.4 GHz with the reduced mutual coupling < -20 dB and peak gain of 3.23 dB for the entire range. Table 1 shows the comparison of the proposed UWB MIMO with the other UWB MIMO in the literature. It shows that the proposed antenna has the advantage in terms of size, bandwidth, isolation, and performance parameters.

4. CONCLUSION

A compact two element hexagon-shaped fractal MIMO antenna is proposed for WLAN applications. The edge-to-edge gap between the radiators is 6 mm, and the size of the design is $44 \times 82\,\text{mm}^2$ with the reduced mutual coupling of less than 20 dB, and gain is positive in the entire range with the peak gain of 3.23 dB obtained. The proposed isolation enhancement technique consists of a stub at the center and a symmetrically placed resistance loaded stub in the ground plane of the MIMO system. The fabricated design is further verified using scattering parameters and radiation performance. A close agreement between the simulated and measured results is observed. Diversity performance for the measured results is calculated where ECC < 0.004, DG > 9.96, CCL < 0.4, and MEG < 3 dB which make the proposed design a good candidate for MIMO UWB antenna for S-band and C-band applications.

REFERENCES

1. Mark, R., N. Rajak, K. Mandal, and S. Das, "Isolation and gain enhancement using metamaterial-based superstrate for MIMO applications," *Radioengineering*, Vol. 28, No. 4, 689–695, 2019.
2. Bhattacharya, A. and B. Roy, "Investigations on an extremely compact MIMO antenna with enhanced isolation and bandwidth," *Microw. Opt. Technol. Lett.*, 1–7, 2019.
3. Tripathi, S., A. Mohan, and S. K. Yadav, "A compact MIMO/diversity antenna with WLAN band-notch characteristics for portable UWB applications," *Progress In Electromagnetics Research C*, Vol. 77, 29–38, 2017.
4. FCC Online Table of Frequency Allocations 47 C.F.R. §2.106 Revised on July 1, 2022.
5. Kumar, A., A. Q. Ansari, B. Kanaujia, J. Kishor, and N. Tewari, "Design of triple-band MIMO antenna with one band-notched characteristic," *Progress In Electromagnetics Research C*, Vol. 86, 41–53, 2018.
6. Sharawi, M. S., "Printed multi-band MIMO antenna systems and their performance metrics [wireless corner]," *IEEE Antennas and Propagation Magazine*, Vol. 55, No. 5, 218–232, Oct. 2013.
7. Sree, G. N. J. and S. Nelaturi, "Design and experimental verification of fractal based MIMO antenna for lower sub 6-GHz 5G applications," *AEU — International Journal of Electronics and Communications*, Vol. 137, 153797, 2021, ISSN1434-8411.
8. Tripathi, S., A. Mohan, and S. Yadav, "A compact octagonal fractal UWB MIMO antenna with WLAN band-rejrction," *Microw. Opt. Technol. Lett.*, Vol. 57, 1919–1925, 2015.
9. Khan, S. B., S. Ghafoor, and K. K. Qureshi, "Mutual coupling reduction using ground stub and EBG in a compact wideband MIMO-antenna," *IEEE Access*, Vol. 9, 40972–40979, 2021.
10. Sakli, H., C. Abdelhamid, C. Essid, and N. Sakli, "Metamaterial-based antenna performance enhancement for MIMO system applications," *IEEE Access*, Vol. 9, 38546–38556, 2021.

11. Liu, R., X. An, H. Zheng, M. Wang, Z. Gao, and E. Li, "Neutralization Line Decoupling Tri-Band Multiple-Input Multiple-Output antenna design," *IEEE Access*, Vol. 8, 27018–27026, 2020.
12. Vasu Babu, K. and B. Anuradha, "Design of Wang shape neutralization line antenna toreduce the mutual coupling in MIMO antennas," *Analog. Integr. Circ. Sig. Process.*, Vol. 101, 67–76, 2019.
13. Zhang, Y.-M., S. Zhang, J.-L. Li, and G. F. Pedersen, "A transmission-line-based decoupling method for MIMO antenna arrays," *IEEE Transactions on Antennas and Propagation*, Vol. 67, No. 5, 3117–3131, May 2019.
14. Gorai, A., A. Dasgupta, and R. Ghatak, "A compact quasi-self-complementary dual band notched UWB MIMO antenna with enhanced isolation using Hilbert fractal slot," *AEU — International Journal of Electronics and Communications*, Vol. 94, 36–41, 2018, ISSN 1434-8411.
15. Abdelgwad, A. H. and M. Ali, "Mutual coupling reduction of a two-element MIMO antenna system using defected ground structure," *2020 IEEE International Symposium on Antennas and Propagation and North American Radio Science Meeting*, 1909–1910, 2020.
16. Chouhan, S., M. Gupta, and D. K. Panda, "Dual band compact antenna with series of hexagonal cut and coupling structure for isolation enhancement," *2017 7th International Conference on Cloud Computing, Data Science & Engineering-Confluence*, 750–753, 2017.
17. Gurjar, R., D. K. Upadyay, B. Kanaujia, and A. Kumar, "A compact U-shaped UWB-MIMO antenna with novel complementary modified Minkowski fractal for isolation enhancement," *Progress In Electromagnetics Research C*, Vol. 107, 81–96, 2021.
18. Rajkumar, S., K. T. Selvan, and P. H. Rao, "Compact 4 element Sierpinski Knopp fractal UWB MIMO antenna with dualband notch," *Microw. Opt. Technol. Lett.*, Vol. 60, 1023–1030, 2018.
19. Weng, W. C. and C. L. Hung, "H-Fractal antenna for multiband applications," *IEEE Antennas Wirel. Propag. Lett.*, Vol. 13, 1705–1708, 2014.
20. Patra, P. K. and M. K. Das, "Modified ground with 50 Ω step fed WLAN notch 2×2 MIMO UWB antenna," *Int. JRF Microw. Comput. Aided Eng.*, 2019.
21. Chandel, R., A. K. Gautam, and K. Rambabu, "Tapered fed compact UWB MIMO diversity antenna with dual band-notched characteristics," *IEEE Transactions on Antennas and Propagation*, Vol. 66, 1677–1684, 2018.
22. Banerjee, J., A. Gorai, and R. Ghatak, "Design and analysis of a compact UWB MIMO antenna incorporating fractal inspired isolation improvement and band rejection structures," *International Journal of Electronics and Communications*, 2020.
23. Chouhan, S., D. K. Panda, V. S. Kushwah, and S. Singhal, "Spider-shaped fractal MIMO antenna for LAN/WiMAX/Wi-Fi/Bluetooth/C-band applications," *AEU — International Journal of Electronics and Communications*, Vol. 110, 152871, 2019, ISSN 1434-8411.
24. Rajkumar, S., N. V. Sivaraman, S. Murali, and K. T. Selvan, "Heptaband swastik arm antenna for MIMO applications," *IET Microw. Antennas Propag.*, Vol. 11, No. 9, 1255–1261, 2017.
25. Sharma, A. and A. Biswas, "Wideband multiple-input-multiple-output dielectric resonator antenna," *IET Microw. Antennas Propag.*, Vol. 11, No. 4, 496–502, 2017.
26. Mei, P., Y.-M. Zhang, and S. Zhang, "Decoupling of a wideband dual-polarized large-scale antenna array with dielectric stubs," *IEEE Transactions on Vehicular Technology*, Vol. 70, No. 8, 7363–7374, Aug. 2021.
27. Hakim, M. L., M. J. Uddin, and M. J. Hoque, "28/38 GHz dual-band microstrip patch antenna with DGS and stub-slot configurations and its 2×2 MIMO antenna design for 5G wireless communication," *2020 IEEE Region 10 Symposium (TENSYMP)*, 56–59, 2020.
28. Yamna, M. B. and H. Sakli, "UWB-MIMO antenna with high isolation using stub dedicated to connected objects," *2020 20th International Conference on Sciences and Techniques of Automatic Control and Computer Engineering (STA)*, 297–300, 2020.
29. Mu, W., H. Lin, Z. Wang, C. Li, M. Yang, W. Nie, and J. Wu, "A flower-shaped miniaturized UWB-MIMO antenna with high isolation," *Electronics*, Vol. 11, No. 14, 2190, 2022.
30. Tang, M.-C., Z. Chen, H. Wang, M. Li, B. Luo, J. Wang, Z. Shi, and R. W. Ziolkowski, "Mutual coupling reduction using meta-structures for wideband, dual-polarized, andhigh-density patch

arrays," *IEEE Transactions on Antennas and Propagation*, Vol. 65, No. 8, 3986–3998, 2017.

31. Park, J.-D., M. Rahman, and H. N. Chen, "Isolation enhancement of wide-band MIMO array antennas utilizing resistive loading," *IEEE Access*, Vol. 7, 81020–81026, 2019.
32. Sharawi, M. S., "Printed multiband MIMO antenna systems and their performance metrics," *IEEE Antennas and Propagation Magazine*, Vol. 55, No. 5, 219–232, 2013.
33. Yadav, D., M. Abegaonkar, S. Koul, V. Tiwari, and D. Bhatnagar, "Two element band-notched UWB MIMO antenna with high and uniform isolation," *Progress In Electromagnetics Research M*, Vol. 63, 119–129, 2017.
34. Zhao, X., S. P. Yeo, and L. C. Ong, "Planar UWB MIMO antenna with pattern diversity and isolation improvement for mobile platform based on the theory of characteristic modes," *IEEE Transactions on Antennas and Propagation*, Vol. 66, No. 1, 420–425, 2018.
35. Singh, H. V. and S. Tripathi, "Compact UWB MIMO antenna with crossshaped unconnected ground stub using characteristic mode analysis," *Microw. Opt. Technol. Lett.*, Vol. 61, No. 7, 1874–1881, Jul. 2019.
36. Sohi, A. K. and A. Kaur, "A complementary Sierpinski gasket fractal antenna array integrated with a complementary Archimedean defected ground structure for portable4G/5G UWB MIMO communication devices," *Microw. Opt. Technol. Lett.*, 1–11, 2020.
37. Bakale, R. S., A. Nandgaonkar, S. Deosarkar, and M. Munde, "Design of ultra-wideband MIMO antenna with dual band elimination characteristics and low mutual coupling," *Progress In Electromagnetics Research C*, Vol. 123, 237–251, 2022.
38. Sharma, M., P. C. Vashist, I. Alsukayti, N. Goyal, D. Anand, and A. H. Mosavi, "A wider impedance bandwidth dual filter symmetrical MIMO antenna for high-speed wideband wireless applications," *Symmetry*, Vol. 14, 29, 2022.
39. Sharma, M., S. Singh, and R. Varma, "Computational design, analysis and characterization of beetle shaped high isolation multiple-input-multiple-output reconfigurable monopole-antenna with dual band filters for wireless applications," *Wireless Pers. Commun.*, Vol. 119, 1029–1049, 2021.